IMA Journal of Mathematical Control and Information (2018) **35**, 1319–1341
doi: 10.1093/imamci/dnx030
Advance Access publication on July 24, 2017

Some stability proofs on proxy-based sliding mode control

RYO KIKUUWE*
Department of Mechanical Engineering, Kyushu University, 744 Motooka, Nishi-ku, Fukuoka 819-0395, Japan
*Corresponding author: kikuuwe@ieee.org

[Received on 2 December 2016; revised on 12 February 2017; accepted on 13 April 2017]

Proxy-based sliding mode control (PSMC) is a control scheme proposed a decade ago originally as a position controller for robot manipulators. This controller has a unique mathematical structure that combines a proportional-integral-derivative (PID) controller and a sliding mode controller in an algebraic way, and has demonstrated its practical usefulness in various applications. Its theoretical foundation, however, has been quite immature. This article presents a set of stability proofs on PSMC as a minimum requirement for future practical applications. Finite-time stability and asymptotic stability of terminal attractors are proven with the use of a non-smooth Lyapunov function.

Keywords: proxy-based sliding mode control; stability proof; finite-time stability; non-smooth Lyapunov function.

1. Introduction

Proxy-based sliding mode control (PSMC) (Kikuuwe & Fujimoto, 2006; Kikuuwe *et al.*, 2010) is a control scheme that has been proposed by the author and his colleagues originally for position control of robotic manipulators. It is an extension of proportional-integral-derivative (PID) position control and also is an approximation of a simple sliding mode control (SMC). Its tracking accuracy is at the same level as PID control as long as the actuator force does not saturate, but it produces smooth, non-overshooting resuming motion from large positional errors resulted from actuator force saturation. After its initial presentation by Kikuuwe & Fujimoto (2006), the practical benefits of PSMC attracted some attentions and many applications from different research groups have been reported, such as rehabilitation robots (Van Damme *et al.*, 2009; Liao *et al.*, 2015; Chen *et al.*, 2016; Jin *et al.*, 2016; Kashiri *et al.*, 2016), piezoelectric nanopositioning systems (Gu *et al.*, 2015), motion platforms (Hastürk *et al.*, 2011; Prieto *et al.*, 2013), bilateral master-slave systems (Nishi & Katsura, 2015), passive actuators (Kashiri *et al.*, 2016), a linear resonant actuator (Yoshimoto *et al.*, 2015) and a liquid-based sensing system (Tanaka *et al.*, 2010). The author and his colleagues have also reported some of its variants (Kikuuwe *et al.*, 2006; Kikuuwe, 2014) and its experimental evaluation in human-robot interaction (Kikuuwe *et al.*, 2008).

In contrast to its practicality, the theoretical backbone of PSMC has been quite immature. A stability analysis has been provided by the author and his colleagues (Kikuuwe *et al.*, 2010, Section 4), but the proof depends on a conjecture, which has not been verified yet. The mathematical structure of PSMC is rather unique. The controller is described as a differential-algebraic inclusion, which involves discontinuity in expression, but it is algebraically equivalent to an ordinary differential equation.

This article presents results of theoretical analysis on properties of PSMC. More specifically, behaviours of PSMC applied to a perturbed one-dimensional second-order system are analysed. Finite-time and asymptotic stability of terminal invariant sets are proven through the use of a non-smooth Lyapunov function.

It should be emphasized that this article is not to present a new controller but to provide a theoretical analysis on an existing controller, namely, PSMC. This article is not either to argue practical advantages of PSMC, but to provide a set of stability proofs as a minimum, baseline requirement for future practical applications of PSMC. Through some experiments presented in our original articles (Kikuuwe & Fujimoto, 2006; Kikuuwe *et al.*, 2010), PSMC has been shown to outperform the conventional boundary-layer implementation of SMC in terms of the tracking accuracy and the insensitivity to the discretization noise of the position measurements. This article however does not intend to discuss this matter in detail.

This article is organized as follows. Section 2 provides some preliminaries, including the overview on PSMC. Section 3 provides the main results, which are stability proofs of PSMC in the continuous-time domain. Section 4 presents some concluding remarks.

2. Background

2.1. *Mathematical preliminaries*

The following scalar functions will be used throughout this article:

$$\mathrm{sgn}(z) \triangleq \begin{cases} z/|z| & \text{if } z \neq 0 \\ [-1,1] & \text{if } z = 0 \end{cases} \tag{2.1}$$

$$\mathrm{sat}(z) \triangleq z/\max(1,|z|). \tag{2.2}$$

Here, it should be noted that the function $\mathrm{sgn}(z)$ is set-valued at $z = 0$. These functions are connected by the following important relation:

$$\forall\{x,y\} \subset \mathbb{R}, \quad y \in \mathrm{sgn}(x-y) \iff y = \mathrm{sat}(x), \tag{2.3}$$

of which the proofs are found in previous articles (Kikuuwe & Fujimoto, 2006; Acary *et al.*, 2012).

Throughout this article, $\partial\mathcal{X}$, $\mathrm{Int}\mathcal{X}$, $\mathrm{cl}\mathcal{X}$ and $\mathrm{cc}\mathcal{X}$ denote the boundary, the interior, the closure and the convex closure of the set $\mathcal{X}$, respectively. The following notation is defined to give the root of a function:

$$\operatorname*{root}_{\xi\in\mathcal{C}} f(\xi) \triangleq \{\xi \in \mathcal{C} | f(\xi) = 0\}. \tag{2.4}$$

In addition, $\|G(s)\|_{\mathcal{L}1}$ is the $\mathcal{L}_1$ gain of the transfer function $G(s)$. (See, e.g. Cao & Hovakimyan, 2008, Definition 2.)

For investigating indifferentiable functions, this paper uses the upper derivative of a function with respect to time, which is defined as follows:

$$D_t^*\Phi(t) \triangleq \lim_{\bar{h}\to+0} \sup_{|h|\leq\bar{h}} \frac{\Phi(t+h)-\Phi(t)}{h}. \tag{2.5}$$

This upper derivative is equal to the (ordinary) derivative if the function $\Phi(t)$ is differentiable.

2.2. *Proxy-based sliding mode control*

PSMC (Kikuuwe & Fujimoto, 2006; Kikuuwe *et al.*, 2010) is a control scheme originally intended for position control of robotic manipulators. In our original contributions (Kikuuwe & Fujimoto, 2006; Kikuuwe *et al.*, 2010), it is implicitly assumed that PSMC is applied to second-order systems, which are roughly described as follows:

$$M\ddot{p}_s = \tau + \phi_s \tag{2.6}$$

where $M > 0$ is the mass of the controlled object, p_s is the position of the object, τ is the actuator force determined by the controller, and ϕ_s is sum of unknown forces from any other sources.

With PSMC, the torque command τ is determined by the following differential-algebraic inclusion (DAI):

$$\tau \in F\mathrm{sgn}(p_d - q + H(\dot{p}_d - \dot{q})) \tag{2.7a}$$

$$\tau = K(q - p_s) + B(\dot{q} - \dot{p}_s) + L\int (q - p_s)dt. \tag{2.7b}$$

Here, p_d is the desired position and q is what we call a 'proxy' position, and $K > 0$, $B > 0$, $L \geq 0$, $H > 0$, and $F > 0$ are all constant scalars that satisfies $KH > B$. The position p_s and the velocity $\dot{p}_s$ are assumed to be available in real-time. A straightforward question that can be raised here is which equation of (2.7a) and (2.7b) determines the controller output τ. The answer is 'both', in the sense that (2.7a) and (2.7b) are a pair of simultaneous equations with two unknowns, τ and $\dot{q}$, and thus τ and $\dot{q}$ are determined so that (2.7a) and (2.7b) are satisfied.

A possible physical interpretation of PSMC (2.7) applied to the system (2.6) is illustrated in Fig. 1. Here, a sliding mode controller, which is represented by (2.7a), applied to the virtual object, i.e. the 'proxy'. Meanwhile, a PID controller, (2.7b), connects the controlled object and the proxy. The outputs of the controllers are both equal to τ, which implies that the proxy is an object that has no mass and that the forces from the two controllers balance each other. Again, the actuator force τ and the proxy velocity $\dot{q}$ are determined so that they satisfy both (2.7a) and (2.7b). Note that setting $L = 0$ means replacing the PID controller by a PD controller. In our previous paper (Kikuuwe *et al.*, 2010), PSMC with $L > 0$ and $L = 0$ are respectively referred to as PID-type PSMC and PD-type PSMC.

It should be noted that the purpose of the controller (2.7) is not to merely stabilize the simple system (2.6). The original articles (Kikuuwe & Fujimoto, 2006; Kikuuwe *et al.*, 2010) intended to eliminate violent overshooting behaviours of position-controlled robots when the actuator forces are saturated and when the position is far separated from the desired position, while preserving the accuracy of position control at the same level as the well-tuned PID controller. The controller (2.7) has been developed based on quite an intuitive consideration using Fig. 1, in which the 'proxy' realizes the ideal 'sliding mode' by completely satisfying $p_d - q + H(\dot{p}_d - \dot{q}) = 0$, and the actual controlled object is restrained to the 'proxy' through the sufficiently stiff PID controller. In the 'sliding mode', the proxy exponentially converges to the desired position without overshoots, and the rate of convergence is adjusted by the parameter H. The sliding-mode-like equation (2.7a) is used not for the robustness purposes, but for realizing the non-overshooting response after actuator force saturation. This means that PSMC (2.7) is not a controller that was built upon a mathematically well-formulated control objective or a particular Lyapunov function. In spite of such ambiguity in the theoretical basis, PSMC has been found useful by some research groups for some real-world applications, especially those involving human–robot interaction, as reviewed in Section I.

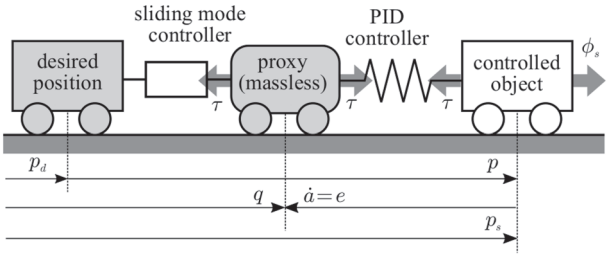

FIG. 1. A physical interpretation of PSMC (2.7) applied to the system (2.6).

For the implementation to digital controllers, the DAI (2.7) is discretized with the implicit Euler method. By the application of (2.3), the discretized form (Kikuuwe *et al.*, 2010, Equation (27)) can be transformed into a closed-form, analytical solution (Kikuuwe *et al.*, 2010, Equation (33)), which can be used as the controller algorithm of PSMC. Details of the derivation can be found in our previous articles (Kikuuwe & Fujimoto, 2006; Kikuuwe *et al.*, 2010).

2.3. *Properties of PSMC*

With the direct application of (2.3), the DAI (2.7), without discretization, can also be converted into another expression having no discontinuities or set-valuedness, which is the following ordinary differential equations:

$$\sigma = p_s - p_d + H(\dot{p}_s - \dot{p}_d) \tag{2.8a}$$

$$\tau = -F\mathrm{sat}\left(\frac{B}{FH}\left(\sigma - \frac{KH-B}{B}\dot{a} - \frac{LH}{B}a\right)\right) \tag{2.8b}$$

$$\ddot{a} = (-K\dot{a} - La + \tau)/B. \tag{2.8c}$$

Here, $\dot{a} \triangleq q - p_s$. The derivation from (2.7) to (2.8) is detailed in Appendix A. It should be emphasized that no approximation intervenes between (2.7) and (2.8) and the apparent algebraic loop through τ in (2.7) is removed thanks to the use of (2.3). The expression (2.8) is convenient for theoretical analysis in the continuous-time domain. Note that the expression (2.8) of the controller does not look like a sliding mode controller anymore, but it is algebraically equivalent to (2.7). The controller (2.8) can be viewed to be in the sliding mode when the right-hand side of (2.8b) is unsaturated, i.e. when

$$\left|\sigma - \frac{KH-B}{B}\dot{a} - \frac{LH}{B}a\right| \leq \frac{FH}{B} \tag{2.9}$$

holds true because the condition (2.9) is equivalent to

$$p_d - q + H(\dot{p}_d - \dot{q}) = 0, \tag{2.10}$$

which results in the set-valuedness of the right-hand side of (2.7a). The equivalence between (2.9) and (2.10) can be seen through the use of (2.8) and (2.3).

The expression (2.8) can be observed from many perspectives. For example, using $\hat{W} \triangleq FH/B$ results in the following expression:

$$\tau = -F\mathrm{sat}\left(\frac{\sigma}{\hat{W}} - \frac{\tau_f}{F}\right) \tag{2.11a}$$

where

$$\mathcal{L}[\tau_f] = \frac{(K - B/H)s + L}{Bs^2 + Ks + L}\mathcal{L}[\tau]. \tag{2.11b}$$

One can see that (2.11), which is equivalent to (2.7), is an approximation of the discontinuous controller

$$\tau = -F\mathrm{sgn}(\sigma), \tag{2.12}$$

which can be obtained by taking the limit of $\hat{W} \to 0$ with (2.11a) in the region of $\sigma \neq 0$. In this extreme case, if there exists an R that satisfies $|\phi_s - M\ddot{p}_d| < R < F$, the sliding mode $\sigma = 0$ takes place in the region $|\dot{p}_s - \dot{p}_d| \leq H(F - R)/M$ (see Appendix B). This justifies the use of the term 'sliding mode' in the name of PSMC as it can be seen as an approximation of SMC. Moreover, (2.11) shows that τ_f is a low-pass filtered value of the actuator force τ. That is, PSMC can be seen as a SMC with a boundary-layer plus low-pass filtered torque feedback. This interpretation contrasts PSMC with a simple output low-pass filtering of SMC, which is one of conventional implementations of SMC.

Another aspect of (2.8) can be made visible by setting $H = B/K$ and $L = 0$, which reduces (2.11a) into

$$\tau = -F\mathrm{sat}(K\sigma/F). \tag{2.13}$$

The controller (2.13) can be viewed as a saturated PD controller whose P and D gains are K and KH, respectively, and also can be viewed as a SMC with a boundary layer whose width is F/K. In this sense, PSMC is a generalization of these schemes. This also justifies the use of 'sliding mode' in the name of the controller (2.8).

Our previous article (Kikuuwe *et al.*, 2010) presented an attempt for the stability proof of PSMC applied to a multi-dimensional second-order mechanical system involving Coriolis and centrifugal terms. In that attempt, the stability is proven based on a conjecture (Kikuuwe *et al.*, 2010, Conjecture 1), which depends on the existence of a strict storage function $V_p(\cdot, \cdot)$ that satisfies the condition presented as equation (45) in Kikuuwe *et al.*'s (2010) article. Unfortunately, such a function has not been found yet. There have been proposed some strict Lyapunov functions as reviewed by Kikuuwe (2013), but they do not satisfy equation (45) in Kikuuwe *et al.*'s (2010) article. Leaving the search for such a function as an open problem, this article focuses on the case with a simple one-dimensional system.

3. Main results

3.1. *The system*

This article considers the system (2.6) controlled with PSMC (2.8) where an extended perturbation $\phi_s - M\ddot{p}_d$ is bounded. By setting $p \triangleq p_s - p_d$ and $\phi \triangleq \phi_s - M\ddot{p}_d$ and specifying the bound of the

extended perturbation, the system considered in this article is now formulated as follows:

$$M\ddot{p} = \tau + \phi \tag{3.1a}$$

$$\tau = -F\,\mathrm{sat}\left(\frac{B}{FH}\left(p + H\dot{p} - \frac{KH - B}{B}\dot{a} - \frac{LH}{B}a\right)\right) \tag{3.1b}$$

$$\ddot{a} = (-K\dot{a} - La + \tau)/B \tag{3.1c}$$

$$|\phi| \leq R_m < R < F \tag{3.1d}$$

where M, K, B, H, F and R are strictly positive constants, L and R_m are non-negative constants and a, p, τ and ϕ are scalar variables. The system (3.1) can be seen as a perturbed position-controlled system that is intended to realize $p \to 0$.

Let us define a vector as follows:

$$x \triangleq \begin{bmatrix} \sigma \\ v \end{bmatrix} \triangleq \begin{bmatrix} p + H\dot{p} \\ \dot{p} \end{bmatrix} \in \mathbb{R}^2. \tag{3.2}$$

In addition, let us define new symbols as follows:

$$\hat{\phi} \triangleq \frac{\phi}{M},\ \hat{F} \triangleq \frac{F}{M},\ \hat{R} \triangleq \frac{R}{M},\ \hat{R}_m \triangleq \frac{R_m}{M},\ \hat{B} \triangleq \frac{B}{K},\ \hat{L} \triangleq \frac{L}{K},\ \hat{W} \triangleq \frac{FH}{B}. \tag{3.3}$$

Then, the system (3.1) can be rewritten as the following state-space representation:

$$\dot{x} = \Psi(x, \hat{\phi} - \hat{F}\rho) \tag{3.4a}$$

$$\rho = \mathrm{sat}((\sigma + \sigma_f)/\hat{W}) \tag{3.4b}$$

$$\begin{bmatrix} \dot{e} \\ \dot{a} \end{bmatrix} = \begin{bmatrix} (-e - \hat{L}a)/\hat{B} - \hat{W}\rho/H \\ e \end{bmatrix} \tag{3.4c}$$

$$\sigma_f = -((H - \hat{B})e + H\hat{L}a)/\hat{B} \tag{3.4d}$$

$$|\hat{\phi}| \leq \hat{R}_m < \hat{R} < \hat{F} \tag{3.4e}$$

where

$$\Psi\left(\begin{bmatrix} \sigma \\ v \end{bmatrix}, \eta\right) \triangleq \begin{bmatrix} v + H\eta \\ \eta \end{bmatrix}. \tag{3.5}$$

Figure 2 illustrates a block diagram of the system (3.4). This system can be seen as a pair of dynamical subsystems, (3.4a) and (3.4c) and (3.4d), interconnected through the static mapping (3.4b), of which the outputs is ρ.

The state vector of the total system (3.4) can be set as the following four-dimensional vector:

$$z \triangleq [x^T, e, a]^T = [\sigma, v, e, a]^T \in \mathbb{R}^4. \tag{3.6}$$

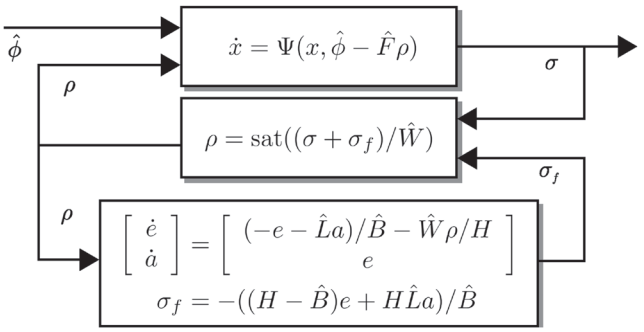

FIG. 2. System (3.4), which represents a perturbed mass controlled with PSMC. Note that $x \triangleq [\sigma, v]^T$.

Then, the system (3.4) can also be written as a saturated linear system of the following form:

$$\dot{z} = \widehat{A}z + \widehat{B}\mathrm{sat}(\widehat{C}^T z) + \widehat{E}\hat{\phi} \tag{3.7}$$

where $\widehat{A} \in \mathbb{R}^{4\times4}$ and $\{\widehat{B}, \widehat{C}, \widehat{E}\} \subset \mathbb{R}^4$ are appropriately chosen matrices and vectors. If there existed a positive definite matrix $P \in \mathbb{R}^{4\times4}$ with which $P(\widehat{A} + \widehat{B}\widehat{C}^T) + (\widehat{A} + \widehat{B}\widehat{C}^T)^T P < 0$ and $P\widehat{A} + \widehat{A}^T P < 0$ are satisfied, the global asymptotic stability and the ultimate boundedness with a bounded $|\hat{\phi}|$ could be obtained. It is however not the case (i.e. such a matrix P does not exist) because the matrices $\widehat{A}$ and $\widehat{A} + \widehat{B}\widehat{C}^T$ do not satisfy the condition provided by Shorten *et al.* (2004, Theorem 2). It has been known that systems of the form (3.7) can be analysed through the conventional Popov and Circle criteria (Khalil, 2002). In addition, some necessary conditions for the stability of systems of the form (3.7) have been provided, e.g. by Hu *et al.* (2002) and Hu *et al.* (2005). These approaches are however difficult to apply to the analytical study on our particular case.

One can see that the system (3.4) is unsaturated and linear in the following subset of the state space:

$$\widehat{\mathcal{S}} \triangleq \left\{ [\sigma, v, e, a]^T \in \mathbb{R}^4 \,\middle|\, |\sigma + \sigma_f| \le \hat{W} \right\}. \tag{3.8}$$

This region is the region in which (2.9), or equivalently, (2.10), is satisfied, and thus is the region in which the proxy is in the sliding mode. The attractively of this set $\widehat{S}$ is of some interest but its proof has not been obtained yet. Therefore, a common approach for sliding mode systems, which usually shows the existence of the sliding mode first and the stability of the origin next, cannot be employed in this paper.

With the use of a simple Lyapunov function, the following limited result is obtained.

THEOREM 3.1 (Global asymptotic stability of the origin of PD-type PSMC with $\hat{\phi} = 0$) Consider the system (3.4a), (3.4b) and (3.4c) and assume that $\hat{L} = 0$ and $\hat{\phi} \equiv 0$. Then, the subspace $\{[x^T, e, a]^T \in \mathbb{R}^4 \,|\, x = 0 \wedge e = 0\}$, which includes the origin, is globally asymptotically stable.

Because a can be practically excluded from the state vector when $\hat{L} = 0$, this theorem states the asymptotic stability of the origin of $\mathbb{R}^3$ (instead of $\mathbb{R}^4$). The proof is shown in Appendix C. Unfortunately, the proof cannot be extended into the PID-type PSMC, i.e. the case of $\hat{L} > 0$. Moreover, the Lyapunov

function used in this proof does not provide appropriate estimate of the domain of attraction in the presence of the disturbance $\hat{\phi} \not\equiv 0$.

Because of the limitations of the aforementioned approaches, we need somewhat non-standard approach, which is presented as follows.

3.2. *Subsystem*

For the convenience of further analysis, we now consider the subsystem (3.4a), of which the state vector is $x \in \mathbb{R}^2$. Equations (3.4c) and (3.4d) imply that ρ and σ_f are linearly connected by the following Laplace-domain representation:

$$\mathcal{L}[\sigma_f] = \hat{W}\mathcal{G}(s)\mathcal{L}[\rho] \tag{3.9}$$

where

$$\mathcal{G}(s) \triangleq \frac{(1-\hat{B}/H)s+\hat{L}}{\hat{B}s^2+s+\hat{L}}. \tag{3.10}$$

The transfer function $\mathcal{G}(s)$ is Hurwitz and thus it is stable in the bounded-input bounded-output sense. Noticing that $|\rho| \leq 1$ is always satisfied, one can see that

$$|\sigma_f|/\hat{W} \leq N_g \triangleq \|\mathcal{G}(s)\|_{\mathcal{L}1} \tag{3.11}$$

is satisfied for all $t \geq 0$. Simple calculus shows that $N_g = 1$ if

$$0 \leq \hat{L} < \frac{H-\hat{B}}{H^2}\left(\leq \frac{1}{4\hat{B}}\right). \tag{3.12}$$

Considering (3.4b), one can find that the boundedness of σ_f directly leads to the state-dependent boundedness of ρ as follows:

$$\rho \in \mathrm{cc}\left(\mathrm{sgn}(\sigma - W) \cup \mathrm{sgn}(\sigma + W)\right) \tag{3.13}$$

where

$$W \triangleq \hat{W}\left(1+N_g\right). \tag{3.14}$$

For the convenience of further discussions, the subsystem (3.4a) combined with the input conditions (3.4e) and (3.13) are now aggregated as follows:

$$\dot{x} = \Psi(x, \hat{\phi} - \hat{F}\rho) \tag{3.15a}$$

$$\rho \in \mathrm{cc}\left(\mathrm{sgn}(\sigma - W) \cup \mathrm{sgn}(\sigma + W)\right) \tag{3.15b}$$

$$|\hat{\phi}| \leq \hat{R}_m < \hat{R} < \hat{F}. \tag{3.15c}$$

In the following, a sufficient condition of the stability of the original system (3.4) is provided through the stability analysis on the subsystem (3.15), which is more tractable.

3.3. *Worst destabilizer candidates*

For the stability analysis of the perturbed system (3.15), we here consider the following autonomous system:

$$\dot{x} = \Psi(x, \hat{\phi} - \hat{F}\rho) \tag{3.16a}$$

$$\rho \in \mathrm{sgn}(\sigma - W\mathrm{sgn}(v)) \tag{3.16b}$$

$$\hat{\phi} \in \hat{R}\mathrm{sgn}(v). \tag{3.16c}$$

The 'artificial' disturbances ρ and $\hat{\phi}$ in (3.16b) and (3.16c) are predicted to pull the state away from the origin marginally outside the conditions (3.15b) and (3.15c), respectively. In this sense, the autonomous system (3.16) exhibits a worse-than-the-worst case scenario of the perturbed system (3.15). An aim of using these 'artificial' disturbances is to derive a Lyapunov function candidate of which the contours coincide (at least partially) with the solution trajectories of this disturbed system. Another aim is to provide an accurate estimate of the domain of attraction based on the inference that, if a solution orbit is a closed curve in the state space $\mathbb{R}^2$, it is on the boundary or in the outside of the domain of attraction.

Let us define the following four subsets of the state space:

$$\mathcal{R}_1 \triangleq \{x \in \mathbb{R}^2 \,|\, \sigma > W \wedge v > 0\} \tag{3.17}$$

$$\mathcal{R}_2 \triangleq \{x \in \mathbb{R}^2 \,|\, \sigma < W \wedge v > 0\} \tag{3.18}$$

$$\mathcal{R}_3 \triangleq -\mathcal{R}_1 = \{x \in \mathbb{R}^2 \,|\, \sigma < -W \wedge v < 0\} \tag{3.19}$$

$$\mathcal{R}_4 \triangleq -\mathcal{R}_2 = \{x \in \mathbb{R}^2 \,|\, \sigma > -W \wedge v < 0\}. \tag{3.20}$$

The disturbances ρ and $\hat{\phi}$ take constant values within the interior of each of the subsets. A careful derivation reveals that, in the regions $\mathcal{R}_i$ ($i \in \{1, \cdots, 4\}$), solution orbits of the autonomous system (3.16) are, respectively, contours of the following functions:

$$G(x) \triangleq \begin{cases} G_1(\mathrm{sgn}(v)x) & \text{if } x \in \mathcal{R}_1 \cup \mathcal{R}_3 \\ G_2(\mathrm{sgn}(v)x) & \text{if } x \in \mathcal{R}_2 \cup \mathcal{R}_4 \end{cases} \tag{3.21}$$

where

$$G_1(x) \triangleq \sigma + \frac{(v - V_y)^2}{2(\hat{F} - \hat{R})} - W \tag{3.22}$$

$$G_2(x) \triangleq -\sigma + \frac{(v + V_w)^2}{2(\hat{F} + \hat{R})} + W - \frac{2\hat{F}^2H^2}{\hat{F} + \hat{R}} \tag{3.23}$$

and

$$V_y \triangleq H(\hat{F} - \hat{R}), \quad V_w \triangleq H(\hat{F} + \hat{R}). \tag{3.24}$$

For the convenience of upcoming derivations, the constant terms of these functions are chosen so that $G_1(x) \geq 0$ for all $x \in \mathcal{R}_1$ and $G_1([W, V_y]^T) = G_2([W, V_y]^T) = 0$.

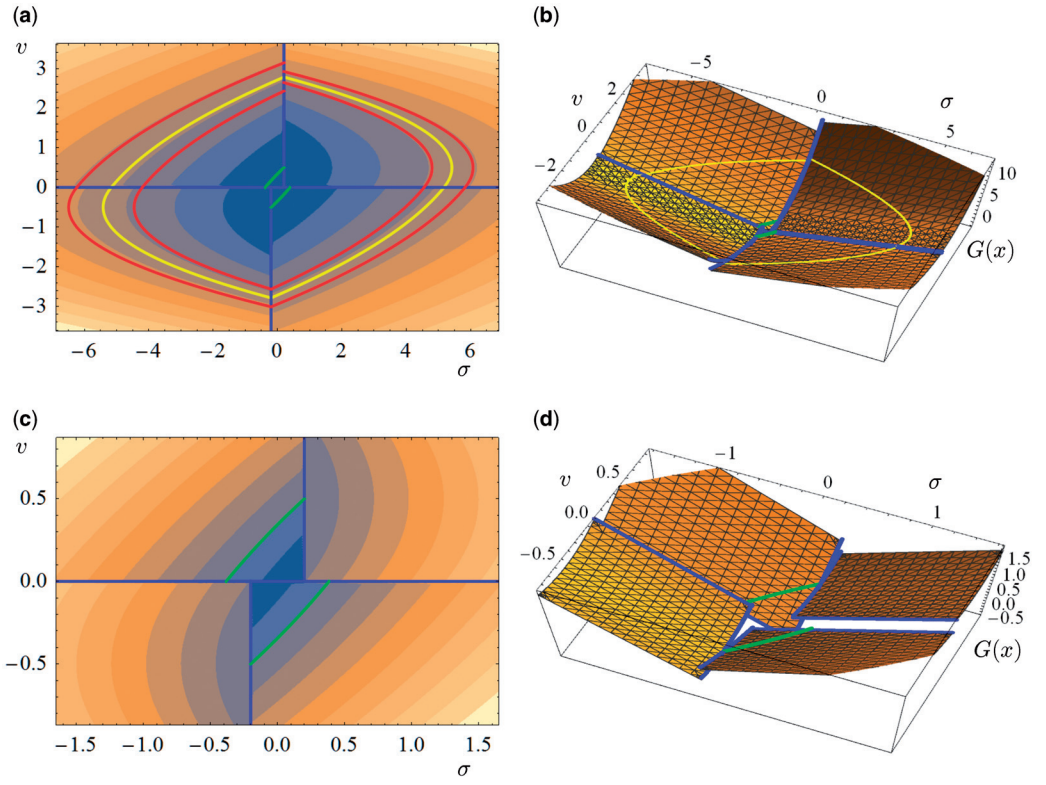

FIG. 3. Plots of $G(x)$ with $\{\hat{F}, H, \hat{R}, W\} = \{1, 1, 0.5, 0.2\}$. In (a), the red and yellow curves are solution orbits of $x(t)$ of the autonomous system (3.16). The yellow one is a closed curve, which bounds the subset $\mathcal{D}$. The blue lines are subsets on which $G(x)$ is discontinuous. The green curves are the contours of $G(x) = 0$. Plots (c) and (d) are enlarged views of (a) and (b), respectively.

Figure 3 shows the plot of function $G(x)$. Figure 3(a) shows examples of solution orbits of the system (3.16), which are composed of contours of $G_i(x)$. These orbits start from the line $\{[W, v]^T | v > 0\}$ and leads clock-wise. The yellow orbit is a special one that forms an closed curve. It can be obtained by the following simultaneous equations with respect to Σ_d and V_d:

$$G_1([W, V_d]^T) = G_1([\Sigma_d, 0]^T) \tag{3.25}$$

$$G_2([W, V_d]^T) = G_2([-\Sigma_d, 0]^T), \tag{3.26}$$

of which the solutions are, if W is small enough, as follows:

$$\Sigma_d \triangleq \frac{\hat{F}H^2(\hat{F}^2 - \hat{R}^2)}{\hat{R}^2}\left(1 + \sqrt{1 - \frac{2\hat{R}W}{H^2(\hat{F}^2 - \hat{R}^2)}}\right)^2 \tag{3.27}$$

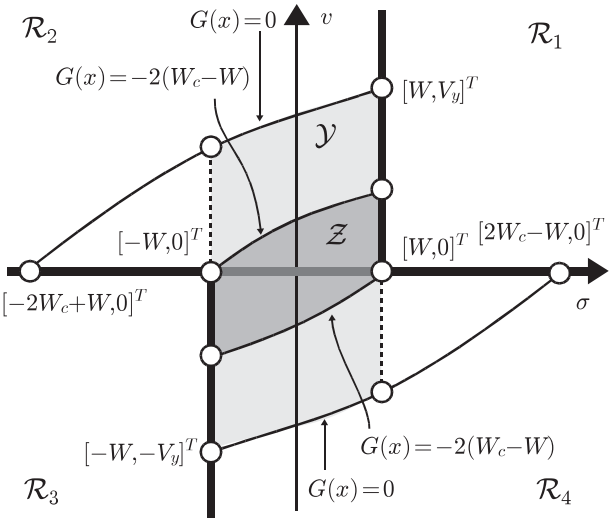

FIG. 4. Some contours and discontinuities of $G(x)$. The thick lines are the subsets on which $G(x)$ is discontinuous.

$$V_d = \frac{H(\hat{F}^2 - \hat{R}^2)}{\hat{R}} \left(1 + \sqrt{1 - \frac{2\hat{R}W}{H^2(\hat{F}^2 - \hat{R}^2)}} \right). \tag{3.28}$$

By using them, we can define the closed set bounded by the closed orbit, which is as follows:

$$\mathcal{D} \triangleq \mathrm{cl}\Big(\left\{ x \in \mathcal{R}_1 \cup \mathcal{R}_3 \,|\, G(x) < G_1([W, V_d]^T) \right\} \\ \cup \left\{ x \in \mathcal{R}_2 \cup \mathcal{R}_4 \,|\, G(x) < G_2([W, V_d]^T) \right\} \Big). \tag{3.29}$$

This set $\mathcal{D}$ is the region enclosed by the yellow curve in Fig. 3(a) and (b). One can see that solutions of the system (3.16) starting inside $\mathcal{D}$ approaches the origin, while those starting outside $\mathcal{D}$ diverge.

Figure 4 shows an enlarged view of the contours of $G(x)$ near the origin. Here, it is assumed that W is small enough to satisfy

$$W < W_c \triangleq \frac{H^2(\hat{F} - \hat{R})(3\hat{F} + \hat{R})}{4(\hat{F} + \hat{R})} \tag{3.30}$$

and the symbols used in the figure are defined as follows:

$$\mathcal{Y} \triangleq \mathrm{cl}\{ x \in \mathcal{R}_2 \cup \mathcal{R}_4 \,|\, |\sigma| \le W \wedge G(x) \le 0 \} \subset \mathbb{R}^2 \tag{3.31}$$

$$\mathcal{Z} \triangleq \mathrm{cl}\{ x \in \mathcal{R}_2 \cup \mathcal{R}_4 \,|\, G(x) \le -2(W_c - W) \} \subset \mathcal{Y}. \tag{3.32}$$

It can be seen that the condition (3.30) is necessary for $\mathcal{Z} \in \mathcal{Y}$ and is sufficient for V_d in (3.28) being a real number.

3.4. *Main results*

The sets $\mathcal{Y}$ and $\mathcal{Z}$ introduced in the previous section have important meanings. A careful observation on the definitions of $\mathcal{Y}$ and $\mathcal{Z}$ shows that, with $W \to +0$, one has

$$\mathcal{Y} \to \mathcal{Y}_0 \triangleq \{x \in \mathbb{R}^2 \,|\, \sigma = 0 \wedge |v| \leq V_y\} \tag{3.33}$$

$$\mathcal{Z} \to \{0\}. \tag{3.34}$$

In this case of $W \to +0$, the system (3.15) reduces to a system with sliding mode that can be described as follows:

$$\dot{x} \in \Psi(x, \hat{\phi} - \hat{F}\,\mathrm{sgn}(\sigma)) \tag{3.35a}$$

$$|\hat{\phi}| \leq \hat{R}_m < \hat{R} < \hat{F}, \tag{3.35b}$$

or equivalently,

$$\dot{p} = v \tag{3.36a}$$

$$\dot{v} \in -\hat{F}\,\mathrm{sgn}(p + Hv) + \hat{\phi} \tag{3.36b}$$

$$|\hat{\phi}| \leq \hat{R}_m < \hat{R} < \hat{F}. \tag{3.36c}$$

It is easy to see that, in the system (3.35), the sliding mode takes place on the line segment $\mathcal{Y}_0$, which can be referred to as a 'sliding patch' (see Appendix B). Moreover, after the state arrives in the sliding patch $\mathcal{Y}_0$, it asymptotically approaches the origin $\{0\} \in \mathbb{R}^2$. In this sense, the sets $\mathcal{Y}$ and $\mathcal{Z}$ are analogous to the sliding patch $\mathcal{Y}_0$ and the origin $\{0\}$, respectively.

The main results on the perturbed subsystem (3.15) are summarized as follows:

THEOREM 3.2 (Finite-time stability of $\mathcal{Y}$) Consider the system (3.15) with W satisfying (3.30). Then, the set $\mathcal{Y}$ is positively invariant and finite-time stable with the domain of attraction including the set $\mathcal{D}$.

THEOREM 3.3 (Asymptotic stability of $\mathcal{Z}$) Consider the system (3.15) with W satisfying (3.30). Then, the set $\mathcal{Z}$, which is a subset of $\mathcal{Y}$, is asymptotically stable with the domain of attraction including the set $\mathcal{D}$.

Proofs are presented in subsequent sections. Due to the definition (3.29) of $\mathcal{D}$, the region of attraction $\mathcal{D}$ in these theorems can be arbitrarily enlarged by increasing $\hat{F}$. Moreover, if there is no disturbance (i.e., $\hat{\phi} \equiv 0$), one can set $\hat{R}_m = 0$ and $\hat{R}$ to be arbitrarily small, and thus the stability of the sets $\mathcal{Y}$ and $\mathcal{Z}$ are given in the global sense.

3.5. *Finite-time stability of $\mathcal{Y}$: proof*

A proof of Theorem 3.2 is now provided. Here we employ a Lyapunov function candidate that partially shares the contours with the function $G(x)$.

Proof of Theorem 3.2. Let us define

$$\alpha \triangleq \frac{\hat{R} - \hat{R}_m}{\hat{F} + \hat{R}} > 0. \tag{3.37}$$

Then, if $x \in \mathrm{cl}(\mathcal{R}_1 \cup \mathcal{R}_3)$, in which $\rho = \mathrm{sgn}(v) = \mathrm{sgn}(\sigma)$, the following is satisfied:

$$\begin{aligned} \dot{G}_1(\mathrm{sgn}(v)x) &= -\frac{|v|(\hat{F}(\mathrm{sgn}(v)\rho - 1) + (\hat{R} - \mathrm{sgn}(v)\hat{\phi}))}{\hat{F} - \hat{R}} \\ &\leq -\alpha \frac{\hat{F} + \hat{R}}{\hat{F} - \hat{R}} |v|. \end{aligned} \tag{3.38}$$

Moreover, if $x \in \mathrm{cl}(\mathcal{R}_2 \cup \mathcal{R}_4)$ and $v \neq 0$,

$$\begin{aligned} \dot{G}_2(\mathrm{sgn}(v)x) &= -\frac{|v|(\hat{F} + \hat{R} + \mathrm{sgn}(v)(\hat{F}\rho - \hat{\phi}))}{\hat{F} + \hat{R}} \\ &\leq -\alpha |v| \end{aligned} \tag{3.39}$$

holds true. These inequalities justify our choice of (3.16b) and (3.16c) as worse-than-the-worst destabilizers because $\dot{G}(x) \leq 0$ always holds true and the equality holds with the disturbances (3.16b) and (3.16c). Moreover, they also suggest that the functions $G_1(\cdot)$ and $G_2(\cdot)$ can be used as building blocks to construct a Lyapunov function of the system (3.15).

Let us construct a Lyapunov function candidate, which is defined as follows:

$$U(x) = \begin{cases} 0 & \text{if } x \in \mathcal{Y} \\ U_1(\mathrm{sgn}(v)x) & \text{if } x \in \mathcal{D}_1 \\ G_2(\mathrm{sgn}(v)x) & \text{if } x \in \mathcal{D}_2 \\ U_5(|\sigma|) & \text{if } x \in \mathcal{D}_3 \end{cases} \tag{3.40}$$

where

$$\begin{aligned} U_1(x) &\triangleq G_2\left(\begin{bmatrix} W \\ \underset{\xi \in [V_y, +\infty)}{\mathrm{root}} (G_1(x) - G_1([W, \xi]^T)) \end{bmatrix}\right) \\ &= \frac{2\hat{F}^2 H^2}{\hat{F} + \hat{R}} \left(\left(1 + \sqrt{\frac{G_1(x)}{2\hat{F}^2 H^2/(\hat{F} - \hat{R})}}\right)^2 - 1\right) \end{aligned} \tag{3.41}$$

$$U_5(\sigma_p) \triangleq U_1(x_\sigma(\sigma_p)) \tag{3.42}$$

$$x_\sigma(\sigma_p) \triangleq \begin{bmatrix} \sigma_p \\ v_\sigma(\sigma_p) \end{bmatrix} \triangleq \begin{bmatrix} \sigma_p \\ \dfrac{\Sigma_d - \sigma_p}{\Sigma_d - W} V_y \end{bmatrix} \tag{3.43}$$

and

$$\mathcal{D}_1 \triangleq \{x \in \mathcal{D}\backslash\mathcal{Y} \,|\, \mathrm{sgn}(v)\sigma \geq W \ \wedge\ |v| \geq v_\sigma(|\sigma|)\} \tag{3.44}$$

$$\mathcal{D}_2 \triangleq \big\{x \in \mathcal{D}\backslash\mathcal{Y} \,|\, |v| \leq W \ \vee \big(\mathrm{sgn}(v)\sigma \leq -W \ \wedge\ G_2(\mathrm{sgn}(v)x) \geq U_5(|\sigma|)\big)\big\} \tag{3.45}$$

$$\mathcal{D}_3 \triangleq (\mathcal{D}\backslash\mathcal{Y})\backslash\mathrm{Int}(\mathcal{D}_1 \cup \mathcal{D}_2). \tag{3.46}$$

Here, $\mathcal{D}_i$ are chosen so that they overlap each other at their boundaries and that $\mathcal{D}_i \cap \mathcal{Y} = \emptyset$ and $\mathcal{D}\backslash\mathcal{Y} = \mathcal{D}_1 \cup \mathcal{D}_2 \cup \mathcal{D}_3$ are satisfied. (Figure 5 illustrates these sets and the function $U(x)$.) The function $U(x)$ is positive definite with respect to the set $\mathcal{Y}$ and is continuous in $\mathcal{D}$. Therefore, the proof can be completed by showing that, for any initial states $x(0) = x_0 \in \mathcal{D}\backslash\mathcal{Y}$, there exists a positive constant $q(x_0)$ such that $D_t^* U(x) \leq -q(x_0)$ for all $t > 0$. (See, e.g. Polyakov & Fridman (2014, Theorem 11).)

If $x \in \mathcal{D}_1 \subset \mathrm{cl}(\mathcal{R}_1 \cup \mathcal{R}_3)$, in which $v \neq 0$, the following is satisfied:

$$\begin{aligned}\dot{U}(x) &= \dot{U}_1(\mathrm{sgn}(v)x)\\ &= \frac{\hat{F}-\hat{R}}{\hat{F}+\hat{R}}\left(\sqrt{\frac{2\hat{F}^2H^2}{G_1(\mathrm{sgn}(v)x)(\hat{F}-\hat{R})}}+1\right)\dot{G}_1(\mathrm{sgn}(v)x)\\ &\leq \frac{\hat{F}-\hat{R}}{\hat{F}+\hat{R}}\dot{G}_1(\mathrm{sgn}(v)x) \leq -\alpha|v| < 0.\end{aligned} \tag{3.47}$$

If $x \in \mathcal{D}_2 \subset \mathrm{cl}(\mathcal{R}_2 \cup \mathcal{R}_4)$, in which $v \neq 0$, the following is satisfied:

$$\dot{U}(x) = \dot{G}_2(\mathrm{sgn}(v)x) < -\alpha|v| < 0. \tag{3.48}$$

If $x \in \mathcal{D}_3$, in which $\mathrm{sgn}(\sigma)v \leq V_y$ and $|\sigma| > W$ are satisfied, the following is satisfied:

$$\begin{aligned}\dot{U}(x) &= \dot{U}_5(|\sigma|)\\ &= \frac{\hat{F}-\hat{R}}{\hat{F}+\hat{R}}\left(\sqrt{\frac{2\hat{F}^2H^2}{G_1(x_\sigma(|\sigma|))(\hat{F}-\hat{R})}}+1\right)\times\\ &\quad\begin{bmatrix}1 & \dfrac{\hat{F}(v_\sigma(|\sigma|)-V_y)}{\hat{F}-\hat{R}}\end{bmatrix}\begin{bmatrix}1\\ -\dfrac{V_y}{\Sigma_d - W}\end{bmatrix}\mathrm{sgn}(\sigma)\dot{\sigma}\\ &\leq -\frac{\hat{F}-\hat{R}}{\hat{F}+\hat{R}}H(\hat{R}-\hat{R}_m) = -\alpha V_y < 0.\end{aligned} \tag{3.49}$$

Therefore, one can see that $U(x)$ is strictly monotonically decreasing in each of the sets $\mathcal{D}_1$, $\mathcal{D}_2$ and $\mathcal{D}_3$. The equality, $\dot{U}(x) = 0$, can hold only on the points $[\pm\Sigma_d, 0]^T$, which are on the boundary of $\mathcal{D}$ but not included in $\mathcal{D}$.

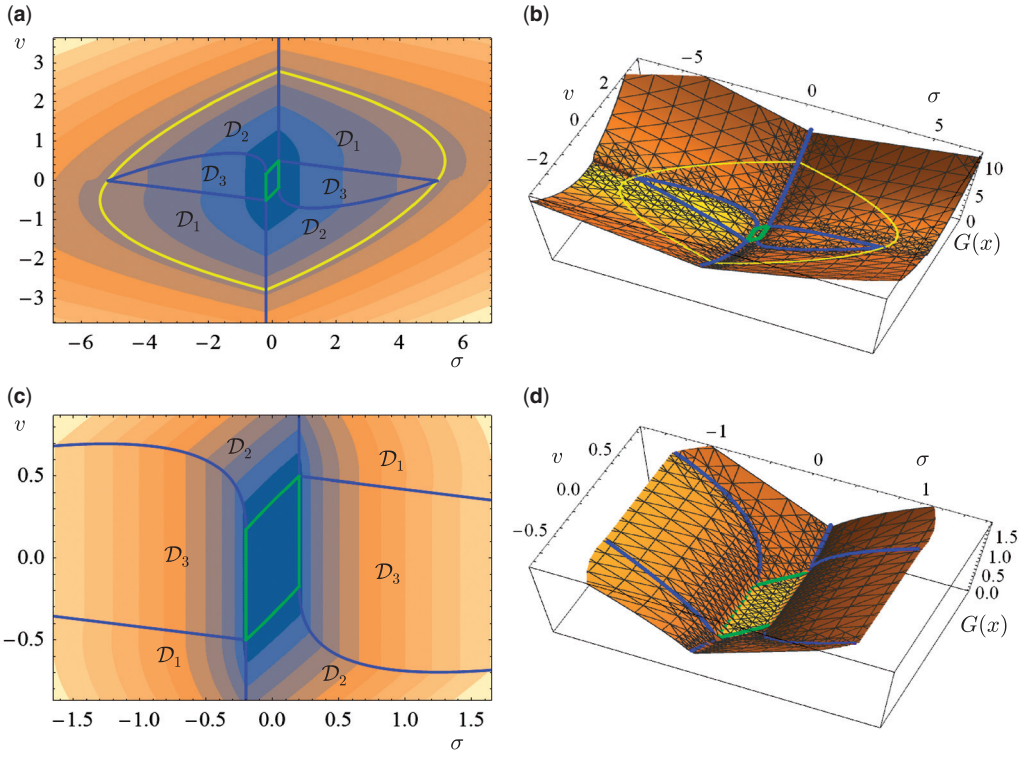

FIG. 5. Plots of $U(x)$ with $\{\hat{F}, H, \hat{R}, W\} = \{1, 1, 0.5, 0.2\}$. Plots (c) and (d) are enlarged views of (a) and (b), respectively. The yellow closed curve represents $U(x) = U([\Sigma_d, 0]^T)$, which bounds the subset $\mathcal{D}$. The blue curves are subsets on which $U(x)$ is indifferentiable. The green curves are the boundary of $\mathcal{Y}$ where $U(x) = 0$.

Due to its definition and due to the fact that $U(x)$ is continuous everywhere, the upper derivative $D_t^* U(x)$ is upperbounded by the derivatives of $\dot{U}(x)$ evaluated in the regions to which x belongs. That is, we have the followings:

$$D_t^* U(x) \leq \dot{G}_1(\mathrm{sgn}(\sigma)x) \leq -\alpha|v| < 0 \quad \text{if } x \in \mathcal{D}_1 \tag{3.50}$$

$$D_t^* U(x) \leq \dot{G}_2(\mathrm{sgn}(v)x) \leq -\alpha|v| < 0 \quad \text{if } x \in \mathcal{D}_2 \tag{3.51}$$

$$D_t^* U(x) \leq \dot{U}_5(|\sigma|) \leq -\alpha V_y < 0 \quad \text{if } x \in \mathcal{D}_3. \tag{3.52}$$

This means that the function $U(x(t))$ strictly monotonically decreases everywhere in $\mathcal{D}\backslash\mathcal{Y} = \mathcal{D}_1 \cup \mathcal{D}_2 \cup \mathcal{D}_3$.

Let us define the function $v_a : \mathbb{R}^2 \to \mathbb{R}$ as follows:

$$v_a(x_0) \stackrel{\Delta}{=} \min_{\substack{x \in \mathcal{D}_1 \cup \mathcal{D}_2 \\ U(x) \leq U(x_0)}} |v|. \tag{3.53}$$

For all $t > 0$ and all initial states $x_0 \in \mathcal{D}\backslash\mathcal{Y}$, $U(x) \leq U(x_0)$ and $0 < v_a(x_0) < V_y$ are satisfied because of (3.50), (3.51) and (3.52). Therefore,

$$D_t^* U(x) \leq -\alpha v_a(x_0) < 0 \tag{3.54}$$

is satisfied for all $t > 0$ and any initial states $x_0 \in \mathcal{D}\backslash\mathcal{Y}$. This concludes the proof. □

REMARK 3.1 By using the function $U(x)$, the definition (3.29) of the set $\mathcal{D}$ can be concisely rewritten as follows:

$$\mathcal{D} = \{x \in \mathbb{R}^2 \mid U(x) < U([\Sigma_d, 0]^T)\}. \tag{3.55}$$

3.6. *Asymptotic stability of $\mathcal{Z}$: proof*

A proof of Theorem 3.3 is now presented. It employs another Lyapunov function, but its choice is relatively easy because the estimated domain of attraction should be only large enough to include an open set including $\mathcal{Y}$, considering that the finite-time reaching to $\mathcal{Y}$ has already been shown by Theorem 3.2.

Proof of Theorem 3.3. Let us define the following Lyapunov function:

$$U_z(x) \triangleq \max(0, U_{z1}(x)) + \max(0, U_{z2}(x)) \tag{3.56}$$

where

$$U_{z1}(x) \triangleq G_2\left(\begin{bmatrix} W\mathrm{sgn}(v)\mathrm{sat}(\sigma/W) \\ |v| \end{bmatrix}\right) + 2(W_c - W) \tag{3.57}$$

$$U_{z2}(x) \triangleq |\sigma| - W. \tag{3.58}$$

The function $U_z(x)$ satisfies $U_z(x) = 0$ if and only if $x \in \mathcal{Z}$, satisfies $U_z(x) \geq 0$ everywhere, and is continuous everywhere. From the definition,

$$\dot{U}_z(x) = \dot{G}_2(\mathrm{sgn}(v)x) < -\alpha|v| \tag{3.59}$$

if $|\sigma| < W$,

$$\dot{U}_z(x) < -\alpha|v| \tag{3.60}$$

also if $|\sigma| > W \wedge v\sigma < 0$, and

$$\begin{aligned} \dot{U}_z(x) &< -\frac{(\hat{R} - \hat{R}_m)(|v| + 2V_w) + 2((\hat{F} + \hat{R})V_y - \hat{R}|v|)}{\hat{F} + \hat{R}} \\ &= -\frac{2\hat{R}}{\hat{F} + \hat{R}}\left(\frac{V_y(\hat{F} + \hat{R})}{\hat{R}} - |v|\right) \end{aligned} \tag{3.61}$$

if $|\sigma| > W \wedge v\sigma > 0$. Therefore, $D_t^* U_z(x) < 0$ is satisfied in the neighbourhood of $\mathcal{Z}$ including $\mathcal{Y}$ and $D_t^* U_z(x) = 0$ may happen only if $v = 0$. At $v = 0$, the definition (3.15a) of the system implies that $\dot{v} = 0$ does not happen. Therefore, invoking LaSalle's invariance theorem, one can find that $\mathcal{Z}$ is asymptotically stable and $\mathcal{Y}$ is a subset of the domain of attraction. Moreover, because Theorem 3.2 states that $\mathcal{Y}$ is finite-time stable with the domain of attraction including $\mathcal{D}$, one can conclude that $\mathcal{Z}$ is asymptotically stable with the domain of attraction including $\mathcal{D}$. □

3.7. *Stability of the total system*

The main subject of this article is the stability of the total system (3.4), which is on the total state space $\mathbb{R}^4$. Theorems 3.2 and 3.3 directly lead to the following result:

THEOREM 3.4 (Stability of PSMC) Consider the system (3.4). Let A_1 and A_2 be defined as follows:

$$A_1 \triangleq \|s\mathcal{G}_2(s)\|_{\mathcal{L}1},\ A_2 \triangleq \|\mathcal{G}_2(s)\|_{\mathcal{L}1} \tag{3.62}$$

where

$$\mathcal{G}_2(s) = 1/(\hat{B}s^2 + s + \hat{L}), \tag{3.63}$$

and let us define the following sets:

$$\widehat{\mathcal{D}} \triangleq \mathcal{D} \times [-A_1, A_1] \times [-A_2, A_2] \subset \mathbb{R}^4 \tag{3.64}$$

$$\widehat{\mathcal{Y}} \triangleq \mathcal{Y} \times [-A_1, A_1] \times [-A_2, A_2] \subset \mathbb{R}^4 \tag{3.65}$$

$$\widehat{\mathcal{Z}} \triangleq \mathcal{Z} \times [-A_1, A_1] \times [-A_2, A_2] \subset \mathbb{R}^4. \tag{3.66}$$

Then, the set $\widehat{\mathcal{Y}}$ is finite-time stable and the set $\widehat{\mathcal{Z}}$ is asymptotically stable with the domain of attraction including $\widehat{\mathcal{D}}$.

Proof. The state-space equation (3.4c) implies that the signal ρ is linearly related to e and a in the following forms:

$$\mathcal{L}[e] = s\mathcal{G}_2(s)\mathcal{L}[\rho], \quad \mathcal{L}[a] = \mathcal{G}_2(s)\mathcal{L}[\rho]. \tag{3.67}$$

From this and from the fact that $|\rho| \leq 1$ for all $t \geq 0$, one can see that, if $|e| \leq A_1$ and $|a| \leq A_2$ are satisfied when $t = 0$, they are also satisfied for all $t > 0$. Considering this fact and Theorems 3.2 and 3.3, one can see that the proof is complete. □

REMARK 3.2 Theorem 3.4 slightly abuses the notion of the asymptotic stability and the finite-time stability because $\widehat{\mathcal{D}}$ shares portions of its boundaries with $\widehat{\mathcal{Y}}$ and $\widehat{\mathcal{Z}}$, not being a superset of neighbourhoods of $\widehat{\mathcal{Y}}$ and $\widehat{\mathcal{Z}}$. It is not however practically important because there is no practical reasons to set the initial values of $[e, a]^T$, which are the controller's internal state variables, outside the region $[-A_1, A_1] \times [-A_2, A_2]$.

The system (3.4), which is equivalent to (3.1), implicitly includes the PID controller (3.1c). From Hurwitz stability criterion, one can see that the stability of the PID-controlled second-order system requires $BK > ML$, which is equivalent to

$$\hat{F}H > \hat{W}\hat{L}. \tag{3.68}$$

Interestingly, the system (3.4) does not require this condition to achieve the asymptotic stability of the set $\widehat{\mathcal{Z}}$. Through a straightforward derivation, one can see that the condition (3.68) is the necessary and sufficient condition of the unsaturated linear system to which the system (3.4) reduces in the subset $\widehat{\mathcal{S}}$. This means that, if the condition (3.68) is violated, the system is unstable in the subset $\widehat{\mathcal{S}}$. Therefore, if the condition (3.68) is violated, the state $z \in \mathbb{R}^4$ will not reach the origin $\{0\} \in \mathbb{R}^4$, which lies in the subset $\widehat{\mathcal{S}}$, although it asymptotically approaches the set $\widehat{\mathcal{Z}}$. This may be able to be seen as a chattering-like behaviour around the origin in the set $\widehat{\mathcal{Z}}$.

If there exists a scalar function $U_o : \mathbb{R}^4 \to \mathbb{R}$ with which $U_o(0) = 0$, $U_o(z) > 0$ and $D_t^* U_o(z) < 0$ for all $z \in \widehat{\mathcal{Z}} \backslash \{0\}$ and with $\hat{\phi} = 0$, the origin $\{0\} \in \mathbb{R}^4$ can be shown to be asymptotically stable with the domain of attraction including $\widehat{\mathcal{D}}$. Such a function would require the condition (3.68) to be negative definite. The quest for such a function U_o is left for future study.

3.8. *Illustrative numerical examples*

Some numerical examples are now presented to illustrate the results of analysis. The simulations are done for the system (3.1), which is a mass (3.1a) under the perturbation (3.1d) controlled with PSMC (3.1b) and (3.1c). In the simulation, the controller (3.1b) and (3.1c) is implemented with the Backward Euler discretization as detailed in our previous articles (Kikuuwe & Fujimoto, 2006; Kikuuwe *et al.*, 2010), and the position p and the velocity v of the mass are updated by the fourth-order Runge Kutta integration of (3.1a). The controlled system (3.1a) is set up as $M = 1$ and $\phi = 0.49 \sin(20\pi t)$ and thus we can set $R = 0.5$. The controller parameters are set as $\{F, H, K, B, L\} = \{1, 1, 100, 10, 200\}$. The timestep size is $T = 0.001$. These settings result in $\{\hat{F}, H, \hat{R}, W\} = \{1, 1, 0.5, 0.2\}$, which is the same setting as Figs 3 and 5.

The results are shown in Fig. 6. It includes the solution trajectories of which the initial values of σ are four different values and the initial values of $\{v, e, a\}$ are zero. Figure 6(a) and (b) shows that all solution trajectories reach the sets $\mathcal{Y}$ and $\mathcal{Z}$, near the origin. Fig. 6(c) shows that the variable $\sigma + \sigma_f$, which appears in (3.4b), converges to the region $|\sigma + \sigma_f| < \hat{W}$, with which the system is unsaturated and linear, and further reduces to the neighbourhood of zero asymptotically. Fig. 6(d) shows asymptotic convergence of the position p to the neighbourhood of zero.

Figure 7 shows another set of numerical results with $L = 2000$, which is 10 times of the case of Fig. 6. This setting does not alter $\{\hat{F}, H, \hat{R}, W\}$ but it violates the condition (3.68). The result shows that there is vibratory behaviour around the set $\widehat{S}$, which can be seen as chattering-like, and thus the origin is not reached. The sets $\mathcal{Y}$ and $\mathcal{Z}$ are, however, reached as implied by Theorems 3.2 and 3.3.

4. Concluding remarks

This article has presented stability analysis on PSMC. A non-smooth Lyapunov function has been employed to provide an accurate estimate of the region of attraction under a bounded disturbance. Two terminal invariant sets have been derived and their finite-time stability and asymptotic stability have been proven. It has been also shown that the terminal invariant sets can be made arbitrarily small by

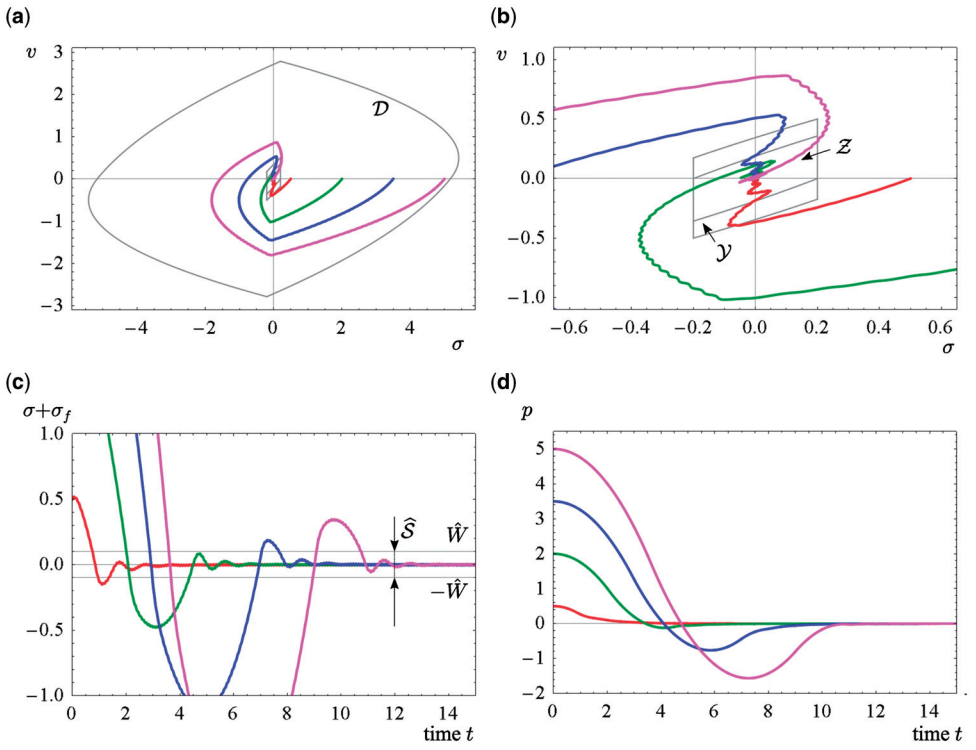

FIG. 6. Illustrative numerical examples of solution trajectories. Thick curves indicate solutions with different initial states. The graph (a) shows the trajectories in the σ-v subspace of the state space. The graph (b) is an enlarged view of the graph (a) and shows that the sets $\mathcal{Y}$ and $\mathcal{Z}$ are reached, as suggested by Theorems 3.2 and 3.3. The graph (c) shows the variable $\sigma + \sigma_f$, indicating that the system reaches $\widehat{\mathcal{S}}$ and is stable therein, which is the consequence of the condition (3.68) being satisfied. The graph (d) shows that the position p asymptotically converges to 0 in any cases.

setting the parameter $\hat{W}$ smaller, and that the domain of attraction can be arbitrarily enlarged by setting $\hat{F}$ higher. The work presented here is limited to a simple one-dimensional case, but many of multi-dimensional mechanical systems can be decoupled into such simple systems when the cross-coupling terms are appropriately bounded, as is the case in robotic manipulators with joint transmissions with high reduction ratios.

As overviewed in Section 1, some research groups have already reported applications of PSMC mainly to position control of robotic devices. The main feature of PSMC that attracted their attention is that PSMC does not produce violent overshooting behaviours when the actuator forces are saturated and when the position is far separated from the desired position. Because the present article has focused only on the stability, the essence of this non-overshooting feature has not been discussed in this article and it still needs more theoretical analysis. The robustness against the measurement noise has been shown only empirically by our original articles (Kikuuwe & Fujimoto, 2006; Kikuuwe *et al.*, 2010) in comparison with the standard boundary-layer implementation of SMC. This robustness may be attributed to the DAI structure (2.7) and to its backward Euler implementation (Kikuuwe & Fujimoto, 2006; Kikuuwe *et al.*, 2010). Theoretical analysis on this matter is still an open problem for future studies.

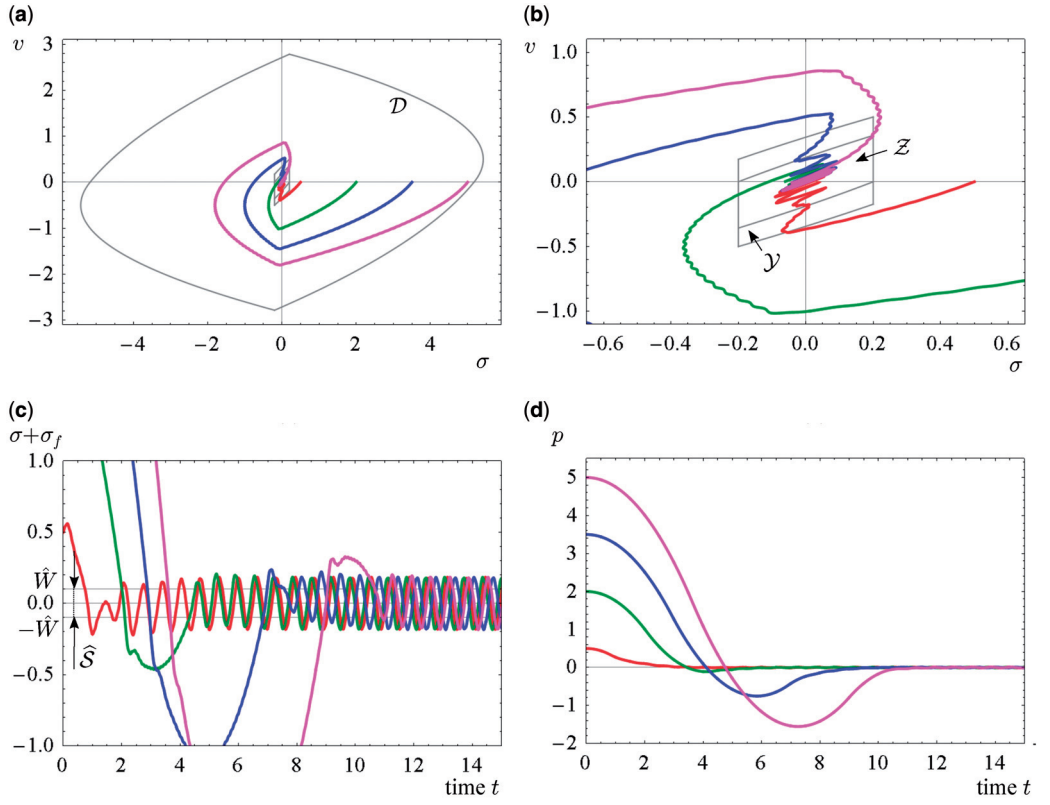

FIG. 7. Numerical example of the same setting as Fig. 6 except a higher value of L, which violates the condition (3.68). The sets $\widehat{\mathcal{Y}}$ and $\widehat{\mathcal{Z}}$ are still stable although the graph of $\sigma + \sigma_f$ shows a persistent oscillatory behaviour, which indicates that the system state does not stay in $\widehat{\mathcal{S}}$.

Funding

This work was supported in part by Grant-in-Aid for Scientific Research (15H03938) from Japan Society for the Promotion of Science (JSPS).

REFERENCES

ACARY, V., BROGLIATO, B. & ORLOV, Y. (2012) Chattering-free digital sliding-mode control with state observer and disturbance rejection. *IEEE Trans. Automat. Control,* **57**, 1087–1101.

CAO, C. & CAO, C. & HOVAKIMYAN, N. (2008) $\mathcal{L}_1$ adaptive controller for systems with unknown time-varying parameters and disturbances in the presence of non-zero trajectory initialization error. *Internat. J. Control,* **81**, 1147–1161.

CHEN, G., ZHOU, Z., VANDERBORGHT, B., WANG, N. & WANG, Q. (2016) Proxy-based sliding mode control of a robotic ankle-foot system for post-stroke rehabilitation. *Adv. Robot.,* **30**, 992–1003.

GU, G.-Y., ZHU, L.-M., SU, C.-Y., DING, H. & FATIKOW, S. (2015) Proxy-based sliding-mode tracking control of piezoelectric-actuated nanopositioning stages. *IEEE/ASME Trans. Mechatronics,* **20**, 1956–1965.

HASTÜRK, Ö., ERKMEN, A. M. & ERKMEN, İ. (2011) Proxy-based sliding mode stabilization of a two-axis gimbaled platform. *Proceedings of the World Congress on Engineering and Computer Science*. pp. 370–376.

Hu, T., Goebel, R., Teel, A. R. & Lin, Z. (2005) Conjugate Lyapunov functions for saturated linear systems. *Automatica,* **41**, 1949–1956.
Hu, T., Lin, Z. & Chen, B. M. (2002) An analysis and design method for linear systems subject to actuator saturation and disturbance. *Automatica,* **38**, 351–359.
Jin, S., Iwamoto, N., Hashimoto, K. & Yamamoto, M. (2016) Experimental evaluation of energy efficiency for a soft wearable robotic suit. *IEEE Trans. Neural Syst. Rehabil. Eng.* doi:10.1109/TNSRE.2016.2613886.
Kashiri, N., Lee, J., Tsagarakis, N. G., Van Damme, M., Vanderborght, B. & Caldwell, D. G. (2016) Proxy-based position control of manipulators with passive compliant actuators: stability analysis and experiments. *Robot. Auton. Syst.,* **75**, 398–408.
Khalil, H. K. (2002) *Nonlinear Systems*, 3rd ed. Prentice Hall, Upper Saddle River.
Kikuuwe, R. (2013) Alternative proofs of four stability properties of rigid link manipulators under PID position control. *Robotica,* **31**, 113–122.
Kikuuwe, R. (2014) A sliding-mode-like position controller for admittance control with bounded actuator force. *IEEE/ASME Trans. Mechatronics,* **19**, 1489–1500.
Kikuuwe, R. & Fujimoto, H. (2006) Proxy-based sliding mode control for accurate and safe position control. *Proceedings of the 2006 IEEE International Conference on Robotics and Automation*. pp. 25–30.
Kikuuwe, R., Yamamoto, T. & Fujimoto, H. (2006) Velocity-bounding stiff position controller. *Proceedings of the 2006 IEEE/RSJ International Conference on Intelligent Robots and Systems*. pp. 3050–3055.
Kikuuwe, R., Yamamoto, T. & Fujimoto, H. (2008) A guideline for low-force robotic guidance for enhancing human performance of positioning and trajectory tracking: it should be stiff and appropriately slow. *IEEE Trans. Syst., Man Cybern. A. Syst. Humans,* **38**, 945–957.
Kikuuwe, R., Yasukouchi, S., Fujimoto, H. & Yamamoto, M. (2010) Proxy-based sliding mode control: a safer extension of PID position control. *IEEE Trans. Robot.,* **26**, 860–873.
Liao, Y., Zhou, Z. & Wang, Q. (2015) BioKEX: A bionic knee exoskeleton with proxy-based sliding mode control. *Proceedings of 2015 IEEE International Conference on Industrial Technology*. pp. 125–130.
Nishi, F. & Katsura, S. (2015) Ultrafine manipulation considering input saturation using proxy-based sliding mode control. *Proceedings of 2015 IEEE International Conference on Mechatronics*. pp. 547–552.
Polyakov, A. & Fridman, L. (2014) Stability notions and Lyapunov functions for sliding mode control systems. *J. Franklin Inst.,* **351**, 1831–1865.
Prieto, P. J., Rubio, E., Hernández, L. & Urquijo, O. (2013) Proxy-based sliding mode control on platform of 3 degree of freedom (3-DOF). *Adv. Robot.,* **27**, 773–784.
Shorten, R. N., Mason, O., O'Cairbre, F. & Paul, C. (2004) A unifying framework for the SISO circle criterion and other quadratic stability criteria. *Internat. J. Control,* **77**, 1–8.
Tanaka, Y., Yu, Q., Doumoto, K., Sano, A., Hayashi, Y., Fujii, M., Kajita, Y., Mizuno, M., Wakabayashi, T. & Fujimoto, H. (2010) Development of a real-time tactile sensing system for brain tumor diagnosis. *Int. J. Comput. Assist. Radiol. Surg.,* **5**, 359–367.
Van Damme, M., Vanderborght, B., Verrelst, B., Van Ham, R., Daerden, F. & Lefeber, D. (2009) Proxy-based sliding mode control of a planar pneumatic manipulator. *Int. J. Robot. Res.,* **28**, 266–284.
Yoshimoto, T., Asai, Y., Hirata, K. & Ota, T. (2015) Dynamic characteristic analysis and experimental verification of 2-DoF resonant actuator under feedback control. *J. Jpn. Soc. Appl. Electromagn. Mech.,* **23**, 521–526.

Appendix A. Derivation from (2.7) to (2.8)

By substituting $q = p + \dot{a}$ to (2.7) and eliminating $\ddot{a}$, one can obtain the following:

$$\tau \in F\mathrm{sgn}\left(-\sigma + \frac{KH - B}{B}\dot{a} + \frac{HL}{B}a - \frac{H\tau}{B}\right) \tag{A.1}$$

where

$$\sigma = p - p_d + H(\dot{p} - \dot{p}_d). \tag{A.2}$$

Here, one can easily see that the sgn(·) function defined in (2.1) has the following property:

$$\mathrm{sgn}(x) = \mathrm{sgn}(cx),\ \forall c > 0,\ \forall x \in \mathbb{R}. \tag{A.3}$$

Thus, (A.1) can be rewritten as follows:

$$\frac{\tau}{F} \in \mathrm{sgn}\left(\frac{B}{FH}\left(-\sigma + \frac{KH - B}{B}\dot{a} + \frac{HL}{B}a\right) - \frac{\tau}{F}\right). \tag{A.4}$$

This expression involves an algebraic loop of τ/F and the set-valuedness, but the direct application of (2.3) shows that (A.4) is analytically equivalent to the following expression:

$$\frac{\tau}{F} = \mathrm{sat}\left(\frac{B}{FH}\left(-\sigma + \frac{KH - B}{B}\dot{a} + \frac{HL}{B}a\right)\right), \tag{A.5}$$

which is free from an algebraic loop or the set-valuedness. Equation (A.5) directly leads to (2.8b).

Appendix B. Existence of sliding mode in simple sliding-mode-controlled system

This appendix section discusses the simple one-dimensional system (2.6) controlled with an ideal sliding mode controller (2.12), which is obtained as a limit of PSMC. Now, such a system can be written as follows:

$$M\ddot{p}_s = -F\mathrm{sgn}(\sigma) + \phi_s \tag{B.1}$$

where

$$\sigma \triangleq p_s - p_d + H(\dot{p}_s - \dot{p}_d). \tag{B.2}$$

Here let us consider the following function:

$$V_s(\sigma) \triangleq \sigma^2/2. \tag{B.3}$$

If there exist R and R_m that satisfy $|\phi_s - M\ddot{p}_d| \le R_m < R < F$ for all $t > 0$, one can see the following:

$$\begin{aligned}\dot{V}_s(\sigma) &= \sigma\left(\dot{p}_s - \dot{p}_d + H\left(-F\mathrm{sgn}(\sigma) + \phi_s - M\ddot{p}_d\right)/M\right)\\ &< -|\sigma|\left(\frac{H(F-R)}{M} - |\dot{p}_s - \dot{p}_d|\right).\end{aligned} \tag{B.4}$$

This indicates that, in the region where $|\dot{p}_s - \dot{p}_d| < H(F-R)/M$ is satisfied, the sliding mode $\sigma = 0$ takes place.

Appendix C. Proof of Theorem 3.1

Proof of Theorem 3.1. Let us consider the following Lyapunov function candidate:

$$U_{pd}(z) = \frac{v^2}{2} + \frac{\hat{F}He^2}{2\hat{B}\hat{W}} + \hat{F}\,|\sigma - Hv + e| \tag{C.1}$$

where $z = [\sigma, v, e]^T \in \mathbb{R}^3$. This function satisfies $U_{pd}(z) > 0$ for all $z \neq 0$ and $U_{pd}(0) = 0$. Its time derivative can be obtained as follows:

$$\begin{aligned}\dot{U}_{pd}(x) = &-\frac{F\hat{W}}{H}\Gamma\left(\frac{\sigma}{\hat{W}} - \frac{(H-\hat{B})e}{\hat{B}\hat{W}}, \frac{\sigma - Hv + e}{\hat{W}}\right)\\ &-\frac{\hat{F}\hat{W}}{H}\left(\mathrm{sat}\left(\frac{\sigma}{\hat{W}} - \frac{(H-\hat{B})e}{\hat{B}\hat{W}}\right) + \frac{He}{\hat{B}\hat{W}}\right)^2\end{aligned} \tag{C.2}$$

where

$$\Gamma(x, y) = (\mathrm{sat}(x) - \mathrm{sgn}(y))(x - \mathrm{sat}(x) - y). \tag{C.3}$$

It is easy to see that this function satisfies $\Gamma(x, y) \geq 0$ for all $\{x, y\} \subset \mathbb{R}$. Therefore, $\dot{U}_{pd}(z) \leq 0$ holds true for all $z \in \mathbb{R}^3$. Here, $\dot{U}_{pd}(z) = 0$ can be satisfied only if

$$e = -\frac{\hat{B}\hat{W}}{H}\mathrm{sat}\left(\frac{H}{\hat{B}\hat{W}}\sigma\right) \tag{C.4}$$

is satisfied. It can be seen that the maximum positively invariant subset of the set $\{z \in \mathbb{R}^3 \mid (C.4)\}$ is the origin. Thus, the origin is globally asymptotically stable. □